*35th EPS Conference on Plasma Phys. Hersonissos, 9 - 13 June 2008 ECA Vol.**32D**, P-2.013 (2008)*

Application of EMC3-EIRENE to NCSX

J. Canik[1], R. Maingi[1], E.A. Unterberg[2], Y. Feng[3], D. Monticello[4], F. Sardei[3], M.C. Zarnstorff[4]

[1]*Oak Ridge National Laboratory, Oak Ridge, USA*

[2]*Oak Ridge Institute for Science and Education, Oak Ridge, USA*

[3]*Max-Planck-Institut für Plasmaphysik, Greifswald/Garching, Germany*

[4]*Princeton Plasma Physics Laboratory, Princeton, USA*

The National Compact Stellarator eXperiment (NCSX) [1] is a quasi-axisymmetric stellarator under construction at the Princeton Plasma Physics Laboratory. The three field-period device has a major radius of 1.4 m and an average aspect ratio of 4.4, with up to 6 MW of neutral beam injection planned. The edge of a typical NCSX magnetic configuration is characterized by a region of stochastic magnetic field lines, with areas of large flux expansion that allow the isolation of plasma-wall interactions. We have investigated the use of toroidally non-continuous target plates to collect the plasma exhaust power; magnetic field line calculations have shown that such a design is capable of intercepting the majority of the power flux [2,3].

As part of the design of plasma facing components for NCSX, the EMC3-EIRENE code [4] has been implemented to model the scrape-off-layer plasma [5]. EMC3 uses a Monte Carlo technique to solve the fluid transport equations in three dimensions and has been coupled to the neutral transport code EIRENE [6], allowing the self consistent calculation of plasma/neutral transport in the scrape-off layer (SOL) and the expected particle and heat fluxes to target plates. In this paper, we present the results of the application of the full set of transport equations in EMC3-EIRENE, including energy, mass, momentum, and impurity transport, to model NCSX SOL plasmas.

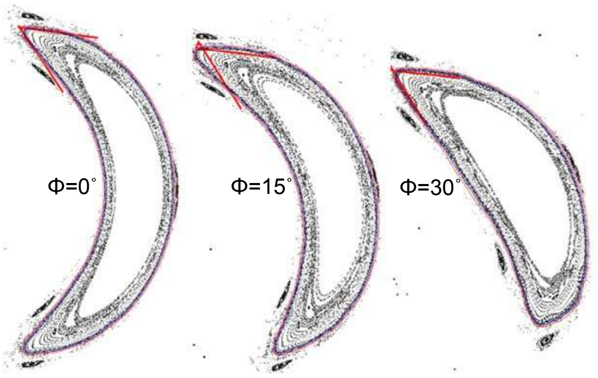

Fig 1: Poincare plots of the magnetic surfaces at toroidal angles of 0,15, and 30°. Also shown are the target plates used in the simulations, which extend from 0 to 30° toroidally

Previously, the electron and ion energy equations were solved with a fixed plasma density, yielding SOL temperature distributions [5]. The magnetic and target geometry (Fig 1) used in the present work are the same as used previously; the magnetic field comes from a PIES [7] calculation of a plasma with $\beta = 4\%$. The targets plates extend 30˚ toroidally within each half-field-period, and penetrate inside otherwise closed flux surfaces, defining a limiter SOL. The rotational transform in the region of the simulations in the range 0.6-0.67; the islands visible just outside the target plates correspond to a transform with a value of 3/5.

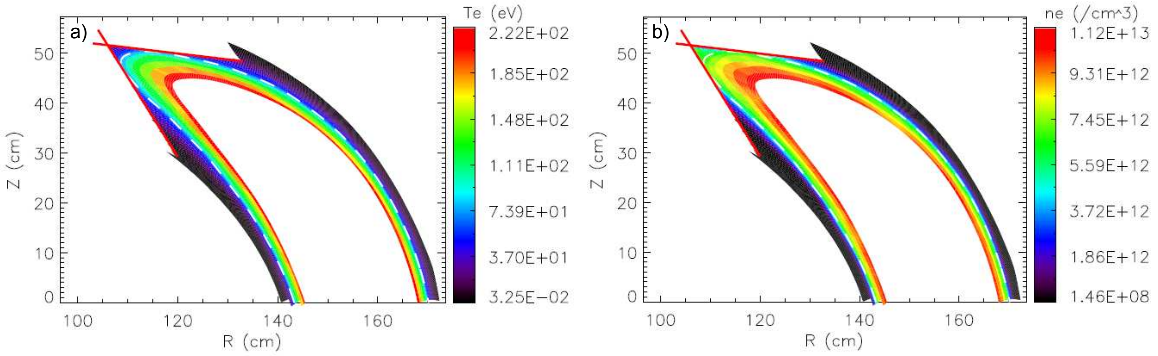

Fig. 2: Electron a) temperature and b) density at $\varphi=18^{\circ}$. Dashed white line is the LCFS.

The electron temperature and density (T_e, n_e) from an EMC3-EIRENE simulation are shown in Figure 2; tests of numerical convergence have been performed with respect to both the number of MC particles tracked and the time steps used, and the typical statistical error in the results shown is ~1%. The input power used in this simulation is 1.2 MW, the density at the innermost grid is set to 10^{13} cm^{-3}, and the cross field transport coefficients are D=1, $\chi_i=\chi_e=3$ m^2/s; these parameters are the same as used in [5], and are used for the sake of comparison. The graphs are shown at a toroidal angle of 18^o, where the targets penetrate most deeply into the core plasma. The dashed white line indicates the last closed flux surface as defined by the target plates. The T_e on this surface is ~80 eV, and is approximately constant just inside this surface. T_e in the SOL is rather high, with a typical value of ~40 eV at the targets. These values are similar to those obtained in [5], where transport was found to be in the sheath-limited regime. The density in the SOL reflects the sheath-limited transport, having fairly low values of ~$5x10^{12}$ cm^{-3} without a strong variation along the LCFS (note that the density does reflect slightly the strong neutral fuelling near the targets).

Calculations of impurity transport have been performed by including carbon sputtering from the target plates, with a constant yield of 2%. The resulting carbon density (Fig. 3a) shows that the SOL provides little shielding of impurities from the main plasma, with the carbon density being highest on the innermost flux surfaces (Z_{eff} in this region is ~1.4).

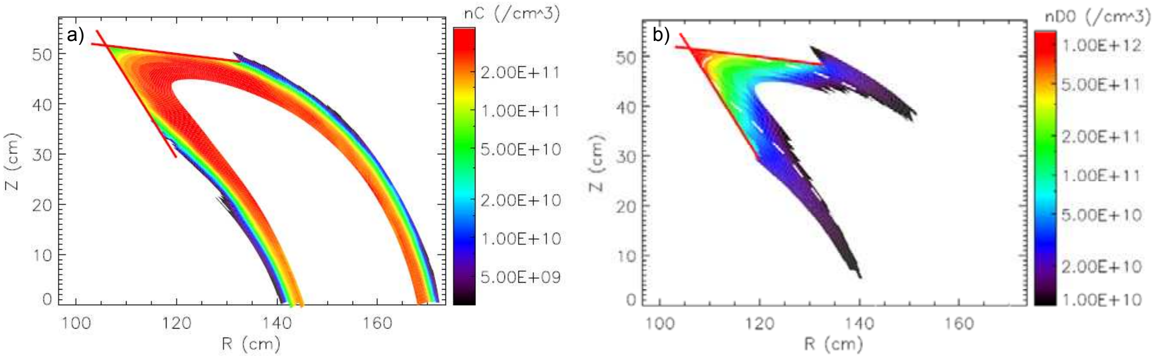

Figure 3: Density of a) carbon and b) neutral hydrogen

Similarly, neutral hydrogen penetration into the core is high, and the density of atomic hydrogen (Fig. 3b) is only reduced by one order of magnitude from the targets to the innermost surface at the poloidal angle of the plates. This is unsurprising since the targets act as limiters, without the shielding advantages of a divertor configuration. Since the plasma n_e in this simulation is low, and the T_e high, the carbon radiation is small; the total radiated power is 40 kW, only 3% of the input power, and so has negligible effect on the plasma temperature.

The calculations indicate that the targets performed well in terms of protecting the vessel wall from the plasma exhaust power; in that only 1.1 kW is absorbed at the wall. The split of the intercepted power between the two plates is fairly even, with the inner plate collecting 60% of the total power and the outer plate 40%. The heat fluxes at the two plates (Fig. 4) show a strong toroidal asymmetry in the deposition profile. This leads to a high value of the peak heat flux, which is ~3.5 MW/m^2 at the inner target and ~2 MW/m^2 at the outer. Although this is not problematic from a power handling standpoint, the input power used in this simulation is only 20% of the planned heating power of NCSX.

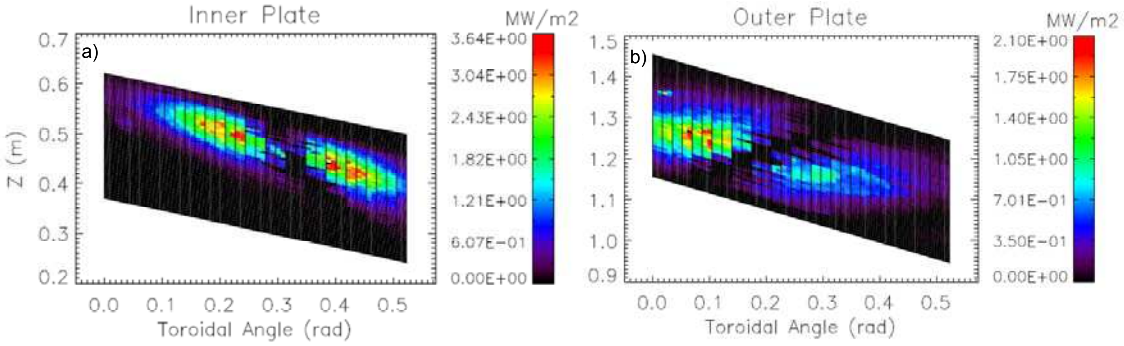

Figure 4: Heat flux at a) inner and b) outer target plates with an inner boundary density of 10^{13} cm^{-3} and input power of 1.2 MW

In order to model a scenario where impurity radiation is non-negligible, a simulation has been performed in which the n_e at the inner boundary is raised to $3\text{x}10^{13}$ cm^{-3}. This caused the typical T_e at the targets to be lowered to ~15 eV. The higher n_e and lower T_e of the

SOL in this case allows for much stronger carbon radiation, which now accounts for ~20% of the input power. The heat fluxes at the targets in this scenario (Fig. 5) show substantially reduced peak values of 1.4 MW/m^2 at the inner and 1.2 MW/m^2 at the outer plate. This is partially due to the broadening of the profiles, as compared to those shown in Fig. 4. This is caused by reduced parallel transport at the lower temperatures, which allows more spreading of the power due to cross-field transport.

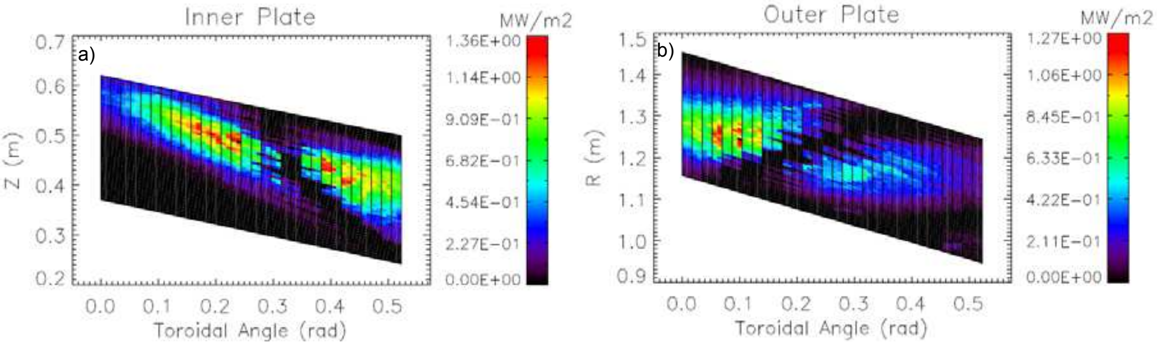

Figure 5: Heat flux at a) inner and b) outer target plates with an inner boundary density of 3x10^{13} cm^{-3} and input power of 1.2 MW

In summary, the application of the EMC3-EIRENE code to the NCSX stellarator has been presented. The full set of transport equations has been implemented, allowing for the self-consistent simulation of the SOL and target deposition. Calculations indicate that the targets are capable of intercepting nearly all of the power and therefore protecting the vessel walls. However, due in part to the toroidal asymmetry of the power deposition, the peak heat fluxes at the plates are rather high. The target plates as simulated act as limiters, and so do not exhibit the neutral and impurity shielding that can be achieved with a divertor configuration. As a next step in the design of PFCs, new target geometries will be modelled that are removed from the closed flux surfaces so that the plasma-material interaction can be isolated from the core plasma.

* Research supported by the US Department of Energy under Contracts DE-AC05-00OR22725 and DE-AC02-76CH03073, in collaboration with IPP-Greifswald.

[1] M. Zarnstorff *et al*, Plasma Phys. Control. Fusion 43, A237 (2001).

[2] T.B. Kaiser, Bull. Am. Phys. Soc. 51, 39 (2006)

[3] R. Maingi, *et al*, Proc. 33rd EPS Conf., Roma, Italy, June 19-23, 2006, paper 5.116

[4] Y. Feng, F. Sardei and J. Kisslinger, J. Nucl. Mater. 266-269, 812 (1999)

[5] F. Sardei *et al,* Proc. 16th Int. Stellarator/Heliotron Workshop, Toki, Japan (2007)

[6] D. Reiter *et al*, Fus. Sci. Technol.47 (2005) 172.

[7] A.H. Reiman, Computer Phys. Comm. 43 (1986) 157.